Helmholtz-Zentrum Dresden-Rossendorf (HZDR)

HELMHOLTZ ZENTRUM
DRESDEN ROSSENDORF

Electronic Properties of a New Family of Layered Materials from Groups 14-15: First-Principles Simulations

Ramzan, M. S.; Bacic, V.; Jing, Y.; Kuc, A.;

Originally published:

September 2019

Journal of Physical Chemistry C 123(2019), 25470-25476

DOI: https://doi.org/10.1021/acs.jpcc.9b07068

Perma-Link to Publication Repository of HZDR:

https://www.hzdr.de/publications/Publ-29488

Release of the secondary publication
on the basis of the German Copyright Law § 38 Section 4.

Electronic Properties of a New Family of Layered Materials from Groups 14-15: First-Principles Simulations

Muhammad Sufyan Ramzan,[1] Vladimir Bacic, [1] Jing Yu, [2,3] and Agnieszka Kuc [1,2,4]

[1] Department of Physics and Earth Sciences, Jacobs University Bremen, Campus Ring 1, 28759 Bremen, Germany
[2] Wilhelm-Ostwald-Institut für Physikalische und Theoretische Chemie, Universität Leipzig, Linnéstr. 2, 04103 Leipzig, Germany
[3] Jiangsu Co-Innovation Centre of Efficient Processing and Utilization of Forest Resources, College of Chemical Engineering, Nanjing Forestry University, Nanjing 210037, China
[4] Helmholtz-Zentrum Dresden-Rossendorf, Forschungsstelle Leipzig, Abteilung Reaktiver Transport, Permoserstr. 15, 04318 Leipzig, Germany

E-mail: a.kuc@hzdr.de

Received xxxxxx
Accepted for publication xxxxxx
Published xxxxxx

Abstract

Variaty of 2D layered materials has gain tremendous focus of materials scientists, physics, chemistry, and other fields of science. This is due to the fact that thin films of layered materials often exhibit superior (for a given application) properties than the parental bulk materials. Thus, in this work, we studied a new family of layered materials with a general composition of XY_3 (where X and Y are elements from Group-14 and 15, respectively). Among the proposed materials, 3D bulk structures of layered GeP_3 and SnP_3 are stable, metallic, and already synthesized in the 1970s. We calculated cleavage energies of mono- and bilayers to be less than 1 J m^{-2}, what indicates possibility of exfoliation from the bulk materials. Many of the investigated monolayers are mechanically and thermally stable. Electronic structure calculations indicate strong interlayer quantum confinement and consequently a metal-to-semiconductor transition when going from bulk to a mono- or bilayer. These electronic properties promise interesting applications in nanoelectronic devices.

Keywords: Novel 2D materials, Group 14-15, density-functional theory, metal-to-semiconductor transition

1. Introduction

Ever since the successful exfoliation of graphene,[1] layered two-dimensional (2D) materials have attracted considerable attention of various fields of science and technology, due to their phenomenal electronic, mechanical, and optical properties[2–4] in the monolayer forms. Up to date, layered materials with different electronic properties are available, ranging from semi-metallic graphene[5–7] to insulating hexagonal boron nitride[8–10] with large variety of semiconducting systems, such as monolayer phosphorous, e.g., black phosphorene,[11] blue phosphorene,[12] and its derivatives,[13–18] transition-metal dichalcogenides (TMDCs) and oxides.[19–21] Ultrahigh carrier mobility of pristine graphene,[22] as high as 10^5 cm^2 V^{-1} s^{-1}, comes with the limitation of the zero band gap. In addition to TMDCs, several derivatives of phosphorene, i.e., GeP_3 (8.84×10^3 cm^2 V^{-1} s^{-1}),[16] InP_3 (1.9×10^3 cm^2 V^{-1} s^{-1}),[15] CaP_3 (~2×10^4 cm^2 V^{-1} s^{-1}),[17] and SnP_3 (1.15×10^4 cm^2 V^{-1} s^{-1}),[18] with finite gaps and high carrier mobilities, have been recently reported. 3D layered materials can be exfoliated to mono- or few-layered system and their properties may strongly differ from these of the parental bulks, and even become superior for different applications.[23] For instance, layered TMDCs from Group 6 show a transition from an indirect band gap in the bulk to a direct band gap character in the monolayers.[24,25]

 © xxxx IOP Publishing Ltd

Recent advancement[26,27] in exfoliation techniques[28–30] and chemical vapour deposition techniques[31,32] motivated material scientists to search for potentially cleavable layered materials.[16,33] Our work is inspired by work of Jing et al.,[16] where the authors reported theoretical cleavage energies of GeP_3 monolayers, potentially enabling exfoliation of this material from its bulk form. Bulk GeP_3 material is known from experiments and its crystal structure was reported in 1970.[34] It is a metallic system, but predicted by Jing et al.,[16] to become semiconducting when thinned to mono- or bilayers, due to a strong vertical quantum confinement.[16] Another experimental work[35] reports on the synthesis of SnP_3, also a Group 14-15 material. Recently, in a theoretical report, Sun et al.,[18] anticipated the metal-to-semiconductor transition for SnP_3, similar to the case of GeP_3, when thinned to monolayers. Moreover, recently predicted potential of GeP_3 for hydrogen evolution reaction (HER),[36] gas sensing applications,[37] and as an excellent anode material for lithium[38] and non-lithium ion batteries[39] ensures that stable XP_3 layers will be a vital addition in the 2D material's zoo. Thus, an obvious question arises weather or not other elements in these groups can exist with the same stoichiometry (XY_3 where X (Group-14) – C, Si, Ge, Sn, Pb and Y (Group-15) – P, As, Sb, Bi) with stable bulk or thin-film forms.

Search for new 2D materials with finite band-gaps for nanoscale (opto)electronic applications is a very active topic. Broad collection of 2D materials can significantly accelerate the advancement in this research area, which is the motivation of our present research. In this work, we investigated the stability and electronic properties of a new class of XY_3 layered materials (where X is an element from Group-14 and Y is an element from Group-15) by means of *ab-initio* calculations. We found that all bulk systems are dynamically stable and exhibit metallic character. Mono- and bilayers have low cleavage energies, however, not all of them are dynamically stable after exfoliation. This may suggest that strong surface reconstruction could occur after exfoliation. All XP_3 systems show relatively good thermal and dynamical stability. Stable monolayers are often semiconducting in contrast to the corresponding bulk forms, which might be interesting for nanoelectronics with single-material logical junctions.

2. Computational Method

All calculations were carried out using density functional theory (DFT) simulations as implemented in the Vienna *ab-initio* simulation package (VASP).[40] We used the projector-augmented wave (PAW) method[41] to describe the electron-nucleus interactions, while generalized-gradient approximation proposed by Perdew, Burke, and Ernzerhof (PBE)[42] was adopted for the exchange and correlation terms, including the dispersion correction D3 approach.[43] Plane-wave cut-off of 500 eV was used. A vacuum region of 15 Å in the *c* lattice direction was inserted to avoid spurious interactions between the periodic images in the slab calculations of mono- and bilayers. All structures were relaxed until all the forces acting on each atom were less than 2×10^{-2} eV Å^{-1} and the total energy change between two self-consistent steps was less than 1×10^{-4} eV. Both lattice vectors and atomic positions were fully relaxed. The Γ–centered *k*-point mesh with 8×8×1 grid was used to sample the Brillouin zone during geometry optimization of bi- (2L) and multilayers (of up to five layers, 5L), while 8×8×8 *k*-mesh for bulk forms in the hexagonal unit cell representation was used (see Figure 1). In order to capture the surface reconstruction that may prevail in the non-planar layered materials,[44] monolayers (1L) were studied also using larger, rectangular unit cells, for which 8×4×1 *k*-mesh was used. We found that this reconstruction, indeed, takes place for single layer systems, where rectangular unit cells with slight out-of-plane distortions of Y atoms have lower formation energies than in the hexagonal representation with no distortions. This reconstruction also affects the electronic properties, as shown in Figure S1 in the Electronic Supplementary Information (ESI) for the exemplary case of 1L GeP_3. On the other hand, such a surface reconstruction was not observed for bi- and multilayer systems. Therefore, in this study, we used the rectangular unit cell representation for the monolayers and hexagonal representation for bi- or multilayer systems. Electronic structures were calculated using both PBE functional (for all systems)[42] and the Heyd-Scuseria-Ernzerhos hybrid functional, HSE06, (for kinetically stable systems).[45] Finite displacement method, as implemented in the Phonopy,[46] was used to calculate the phonon dispersion relations, in order to check the

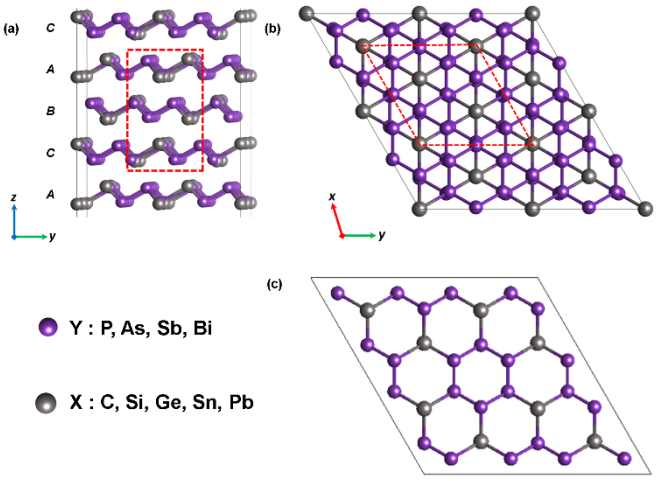

Figure 1 *Crystal structures of bulk XY_3 systems in the 2×2×2 supercell representation: (a) side and (b) top views. Purple and grey represent Y and X atoms, respectively. (c) Top view of a XY_3 monolayer. Figures were created using 3D visualization package VESTA.[54]*

dynamical stabilities. These were performed using $8\times2\times1$, $3\times3\times1$, and $3\times3\times3$ k-meshe grids for 1L, 2L, and bulk systems, respectively. *Ab-initio* molecular dynamics (AIMD) simulations within the NVT ensemble were performed in order to check the thermal stabilities of the XP_3 monolayers. For AIMD calculations, a 3×3 supercell was used to lift the constraint of the unit cells and 400 K (or 300 K) temperature was held for 10 ps with the time step of 1 fs controlled via Nosé–Hoover thermostat.[47] For details on the cleavage energy calculations see ESI.

3. Results and Discussion

3.1 Structural properties of bulk materials

The crystal structures of bulk XY_3 (see Figure 1) belong to the $R\bar{3}m$ space group. The calculated lattice parameters of XP_3 systems are listed in Table 1 together with the interlayer distances, while selected bond lengths are given in Table S1 (see Tables S2 and S3 in ESI for the data on the XAs_3 and XSb_3 materials). Our relaxed lattice parameters for bulk GeP_3 and SnP_3 are $a = b = 7.088$ Å, $c = 9.830$ Å and $a = b = 7.422$ Å, $c = 10.550$ Å, respectively, which are in a good agreement with the experimentally obtained bulk systems ($a = b = 7.050$ Å, $c = 9.930$ Å for GeP_3 and $a = b = 7.380$ Å, $c = 10.510$ Å for SnP_3).[34,35] Figures 1(a) and 1(b) show the top and side views of the XY_3 crystal bulk structure, where the layers are stacked in the *ABCABC* order. Figure 1c shows the corresponding top view of a monolayer. In each layer, atoms are placed in the two adjacent hexagonal planes such that they form a phosphorene-like puckered structure, where each P atom is bound with two neighbouring P atoms and one X atom. Each X atom forms three X─P bonds with three neighbouring P atoms. The in-plane lattice parameters increase with heavier element, as expected, for all the layered forms, 1L, 2L, and bulk. This is due to the strong variation of the X─P bond lengths. Except for CP_3, also the interlayer distances increase for the heavier elements. The apparent difference in the CP_3 structure comes from the fact that C atoms are smaller than P atoms and, thus, the interlayer distance is rather defined by the distance between P atoms in the adjacent layers than between X atoms, as it is in the other XP_3 systems.

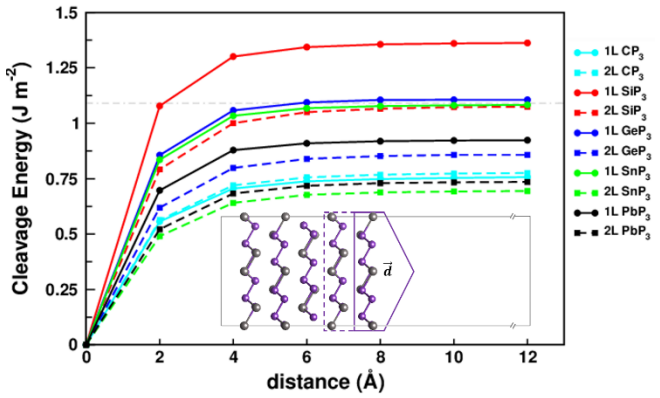

Figure 2 *Calculated cleavage energies of XP_3 (X – C, Si, Ge, Sn, Pb) 1L and 2L shown as solid and dashed lines, respectively, as function of the separation distance between 1L or 2L and the remainder of 5L slab. The distance zero refers to the equilibrium distance of bulk-like 5L-slab. Grey dashed line indicates the threshold energy for mechanically cleavable materials. The calculated cleavage energies fall below or about the threshold, suggesting that all systems, except 1L SiP_3, should be cleavable from their bulk or multilayer stacks.*

3.2 Cleavage energies of 1L and 2L from bulk

Primarily, exfoliating mono- or few-layers from layered bulk materials is realizable by micromechanical cleavage or liquid exfoliation techniques, if the cleavage energy is equal or less than about 1 J m^{-2}.[28,48] To assess the possibility of mono- and bilayer exfoliation from multilayer (or bulk) XP_3, we estimated the cleavage energies (see Figure 2 and ESI for calculation details) for both 1L and 2L XP_3 from a bulk-like 5L-slab model, as shown in the inset of Figure 2. Threshold cleavage energy of the mechanical or liquid exfoliation methods is indicated with a grey dashed line. We found that all 1L and 2L XP_3 fall below the threshold limit, making them potentially cleavable, except for 1L SiP_3 (i.e. 1.36 J m^{-2}), however, this material is the only unstable 1L XP_3 system (see Section 3.3). For comparison, theoretically estimated exfoliation energies of MoS_2,[49] graphene,[50] 1L SnP_3,[18] 1L GeP_3,[16] and 1L InP_3[15] are 0.29 J m^{-2}, 0.32 J m^{-2}, 0.71 J m^{-2}, 1.14 J m^{-2}, and 1.32 J m^{-2}, respectively.

Table 1 *Calculated lattice parameters of XP_3 (with X – C, Si, Ge, Sn, Pb) mono- (a, b), bilayers (a, b), and bulk (a, b, c) forms. For monolayer (1L), a and b lattice parameters are given for the rectangular unit cell representation, while for bilayer (2L) and bulk, hexagonal unit cells were used. Interlayer distances (d) along the z-axis are given for 2L and bulks.*

System	*Lattice vectors* (Å)			*d* (Å)	
	1L *rectangular(a, b)*	2L *hexagonal(a=b)*	Bulk *hexagonal(a=b, c)*	2L	Bulk
CP_3	6.234, 10.806	6.215	6.243, 10.438	2.272	2.201
SiP_3	6.838, 11.841	6.793	6.938, 8.927	1.742	1.697
GeP_3	6.960, 12.055	6.958	7.088, 9.830	1.925	1.886
SnP_3	7.156, 12.387	7.252	7.422, 10.550	1.894	1.886
PbP_3	7.292, 12.613	7.418	7.685, 10.856	1.937	1.982

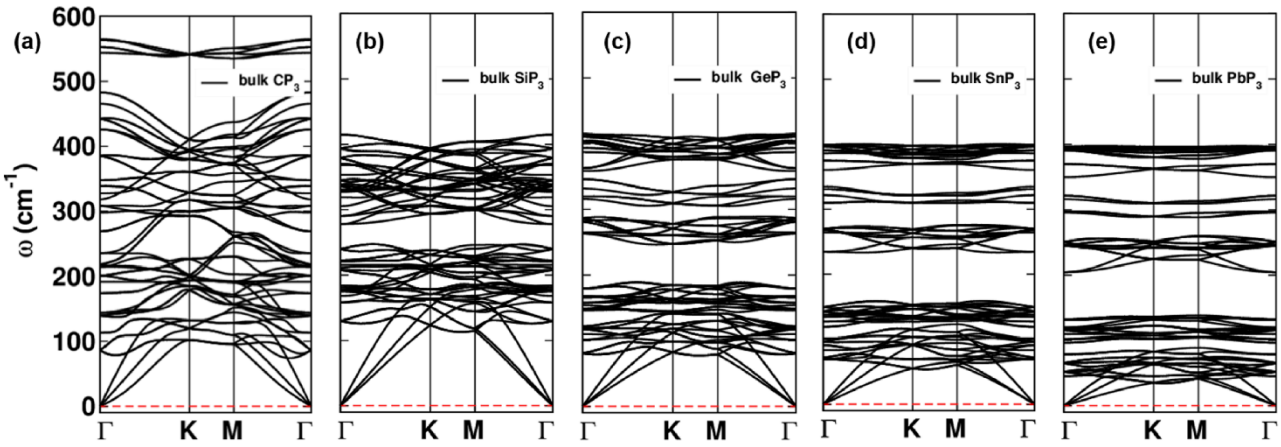

Figure 3 *Calculated phonon dispersion relations of bulk (a) CP_3, (b) SiP_3, (c) GeP_3, (d) SnP_3, and (e) PbP_3 using 2×2×2 supercells.*

The differences between the cleavage energies of 1L (solid lines) and 2L (dashed lines) indicate the material's affinity to be exfoliated either as mono- or bilayers, respectively. For example, 2L SnP_3 should be easier to exfoliate than 1L, whereas, for CP_3, these energies are very similar, indicating that both forms could be obtained (cf. Figure 2). The corresponding data for XAs_3 and XSb_3 are shown in Figure S3. In these cases, the cleavage energies for

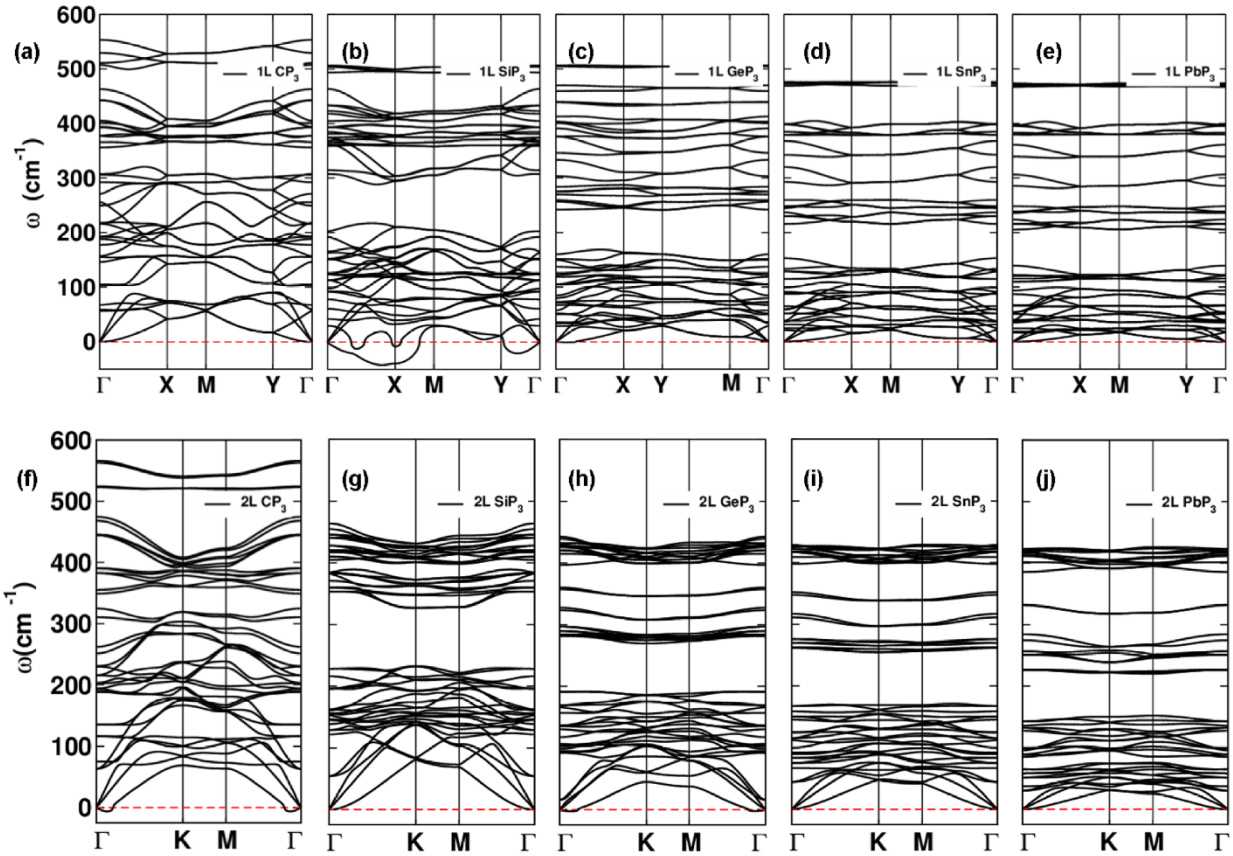

Figure 4 *Phonon dispersion relations of monolayer (a) CP_3, (b) SiP_3, (c) GeP_3, (d) SnP_3, and (e) PbP_3 with 5×2×1 supercells for all systems, except 1L CP_3, for which we used 6×2×1 supercell. (f) – (j) Phonon dispersion relations of bilayer XP_3 with 3×3×1 supercells.*

all systems fall below the threshold, however, as it is discussed in Section 3.3, not all 1L and 2L of XAs_3 and XSb_3 are dynamically stable.

3.3 Phonon dispersion relation

Next, we have investigated the stability of bulk and exfoliated 1L and 2L systems. For this, we have calculated the phonon dispersion relations. All bulk XY_3 systems are stable with real frequencies throughout the Brillouin zone, as shown in Figure 3 (refer to Figure S2 for bulk XAs_3 and XSb_3). The same simulations were performed to check the stability of the exfoliated layers. Figure 4 shows the phonon dispersion relations of 1L and 2L XP_3 (refer to Figures S4 and S5 for the other materials). Due to the surface reconstruction in the monolayers, much larger supercells are required to correctly calculate the phonons. Since degree of reconstruction is not the same in each system, the required supercells are, therefore, different. For instance, 6×2×1 supercell is needed to accurately calculate phonons of 1L CP_3, while 5×2×1 supercells is sufficient for other XP_3 systems. All real phonon branches indicate mechanical stability of all monolayers, except for SiP_3, which has imaginary modes in the entire Brillouin zone, as shown in Figure 4(b). This may suggest either instability of such a monolayer or that the material may undergo yet another type of reconstruction (not taken into account in this study).

The results of 2L XP_3 systems indicate that all bilayers are fairly stable. Very small imaginary frequencies close to the Γ point (e.g., for 2L CP_3) stem from too small unit cells used in the finite displacement calculations of phonons and could be removed by extension of the unit cell size. Larger supercells are, however, computationally too demanding and not affordable with our present resources, but our conclusions should be sound.

While most of the 1L and 2L systems of XP_3 seem to be stable, the corresponding XAs_3 and XSb_3 are not. Taking into account the unit cell size argument, we can conclude that the only stable materials are 1L CAs_3 (CSb_3) and $GeAs_3$ ($GeSb_3$), and 2L CAs_3 (CSb_3) and $SnAs_3$ ($SnSb_3$). All the other systems could be argued that another type of reconstruction is necessary to stabilize them. On the other hand, we have not considered thicker films, e.g., 3L, which might be kinetically stable.

To assess the thermal stability of 1L XP_3 systems, we

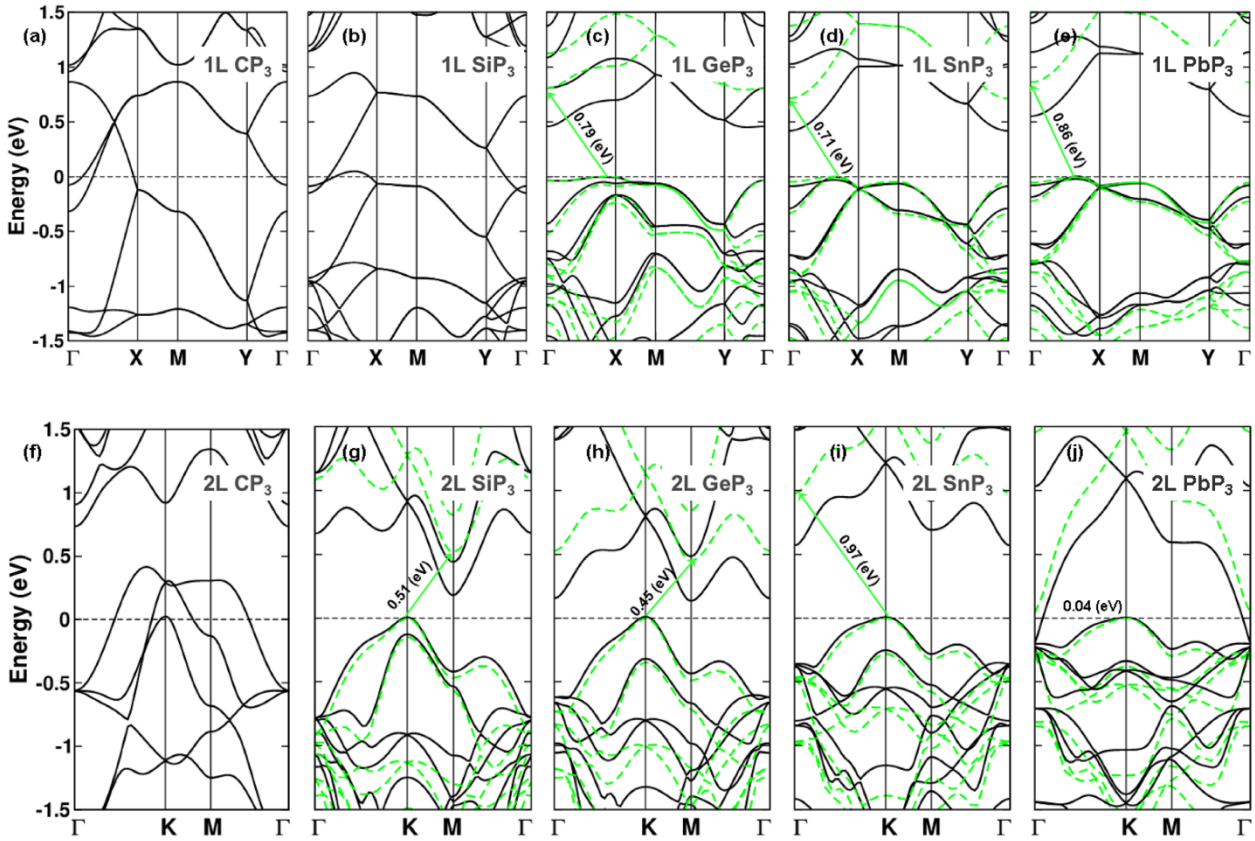

Figure 5 *Band structures of (a) – (e) monolayer and (f) − (j) bilayer CP_3, SiP_3, GeP_3, SnP_3, and PbP_3 respectively, calculated at the PBE (solid black) and HSE06 (dashed green) levels of theory. The horizontal dash lines indicate the Fermi levels, which for practical reasons were shifted to zero. For semiconducting systems, the Fermi levels are additionally shifted to the top of the valence bands.*

performed molecular dynamics simulations at 300 K and 400 K (see Figures S6-S11). Similar to the results of phonons, all the 1L XP_3 are thermally stable at 300 K, while at 400 K, CP_3 and SiP_3 show some instability, indicating that synthesis of these materials as monolayers, should be implemented at ambient conditions.

3.4 Electronic properties

All bulk XY_3 (Y – P, As, Sb) systems are metallic, as shown in Figure S12. Our expectation was that in most of the cases, if not all, a metal-to-semiconductor transition will occur, when reducing the number of layers from bulk down to bi- or monolayers. While this expectation proofed correct for XP_3 systems, it completely failed for XSb_3. For As-based system, only a few materials became semiconducting under such a confinement.

We found that most P-based systems in 1L and 2L forms are semiconductors, while systems with three or more layers are essentially metallic or semi-metallic. Both PBE and HSE06 levels of theory predict the same band-gap character of all semiconducting system, with the former method underestimating the band gap values by maximum of 0.34 eV for 1L GeP_3 (see Figure 5). In details: Monolayers of CP_3 and SiP_3 are metallic, while monolayers of GeP_3, SnP_3, and PbP_3 are semiconducting. Interestingly, 2L SiP_3 is semiconducting, while its single layer is metallic. This also indicates that 1L SiP_3 may be unstable in the present configuration and another surface reconstruction might be more favourable. This is in accordance with the phonon dispersion relations for both systems (cf. Figure 4(b) and (g)), in which 2L SiP_3 is stable, while 1L is not. For CP_3, both 1L and 2L forms are metallic, while the heaviest PbP_3 as 2L has a very small band gap of about 38 meV. All semiconducting systems are indirect band gap materials, with band gaps below 1 eV.

For the heavier elements, such as Ge, Sn or Pb, we have recalculated the band structures of monolayers with spin-orbit coupling (SOC), however, no significant changes in the band structures and band gaps were observed. Negligible SOC in 1L XP_3 may be related to the stoichiometry, where heavier elements account for only 25% of the whole structure. Furthermore, partial density of states (PDOS), as shown in Figure S13, with indicated frontier bands (i.e. valence band maximum, VBM, and conduction band minimum, CBM) are predominantly formed by the P and X atom 2*p*-orbitals.

The electronic structures of As- and Sb-based 1L and 2L systems are shown in Figures S14 and S15. The stable 2L $SnAs_3$ and $SnSb_3$ systems become semiconducting, however, the latter's band gap is only about 50 meV. We expect that for 2L $GeAs_3$ and $PbAs_3$, the semi-metallic character obtained at the PBE level might in fact become semiconducting (similar to 1L forms), if treated at the HES06 level. These systems are, however, kinetically unstable, what was shown in the phonon dispersion calculations, thus, band structures were not recalculated with the more expensive HSE06 (cf. Figure S4).

Applying tensile strain or compression can modulate electronics of 2D layered materials. Here, we show the effect of compressive and tensile strain on the band structures of 1L SnP_3 and 1L PbP_3, as exemplary materials (see Figure S16). This effect in 1L GeP_3 has already been studied and reported earlier.[16] Both layers stay in-direct gap semiconductors under strain, though direct gap at the Γ point is very close, at 5% strain, it is only 8 meV below. Moreover, opposite to effects observed in transition-metal dichalcogenides, e.g., MoS_2,[51] the band gap increases with increasing strain and decreases under compression. The same phenomenon was observed for 1L GeP_3.[16]

Thickness dependent electronic properties of the proposed materials could make it possible to fabricate devices on a single material. For example, field effect transistors with metallic electrode made of few-layer materials and the semiconductor channel of a monolayer of the same material, as proposed earlier for other layered systems.[52,53] This new family of Group 14-15 materials shows potential for such applications. Furthermore, unique crystal structure of few layers XY_3 anticipates a potential application in gas sensing and hydrogen evolution reactions, as reported already for GeP_3.[36,37]

4. Conclusion

In conclusion, we report on a new class of layered materials, XY_3 (X – Group-14, Y – Group-15 element), where metallic bulks turn to semiconducting 1L and 2L systems, indicating a strong vertical quantum confinement effects. Small cleavage energies of 1L and 2L forms, less than 1 J m^{-2}, suggest the possibility of exfoliation from the corresponding bulk or multilayer phases. All bulk materials and most of the proposed 1L and 2L structures are kinetically and thermally stable. Monolayers, however, undergo surface reconstruction, which has to be taken into account with care, when optimizing their geometries. Surface reconstruction also affects the electronics of 1L forms. Surfaces of bi- and multi-layers are not a subject to such a reconstruction. Many 1L and 2L system become semiconducting, with band gaps below 1 eV, while all the bulk systems are metallic. Moreover, the band gaps of 1L and 2L materials could be tuned by tensile strain or compression, because they increase while the material is strained and decrease when it is compressed. If the film thickness of these materials could be experimentally controlled, this new family of 2D materials would be available to fabricate unique devices, e.g., transistors built from a single material, which would strongly reduce the power losses at the electrode-channel junctions.

Acknowledgements

Financial support by the Deutsche Forschungsgemeinschaft (GRK 2247/1 (QM3)) and the high-performance computing resources of ZIH Dresden are gratefully acknowledged. The authors thank Prof. Thomas Heine for his insightful comments and fruitful discussions.

References

[1] Novoselov K S, Geim A K, Morozov S V., Jiang D, Zhang Y, Dubonos S V., Grigorieva I V. and Firsov A A 2004 Electric field in atomically thin carbon films *Science (80-.).* **306** 666–9

[2] Wang Q H, Kalantar-Zadeh K, Kis A, Coleman J N and Strano M S 2012 Electronics and optoelectronics of two-dimensional transition metal dichalcogenides *Nat. Nanotechnol.* **7** 699–712

[3] Qian X, Liu J, Fu L and Li J 2014 Quantum spin Hall effect in two-dimensional transition metal dichalcogenides *Science (80-.).* **346** 1344–7

[4] Singh A K, Mathew K, Zhuang H L and Hennig R G 2015 Computational screening of 2D materials for photocatalysis *J. Phys. Chem. Lett.* **6** 1087–98

[5] Castro Neto A H, Guinea F, Peres N M R, Novoselov K S and Geim A K 2009 The electronic properties of graphene *Rev. Mod. Phys.* **81** 109–62

[6] Allen M J, Tung V C and Kaner R B 2010 Honeycomb Carbon: A Review of Graphene *Chem. Rev.* **110** 132–45

[7] Avouris P 2010 Graphene: Electronic and Photonic Properties and Devices *Nano Lett.* **10** 4285–94

[8] Nag A, Raidongia K, Hembram K P S S, Datta R, Waghmare U V. and Rao C N R 2010 Graphene Analogues of BN: Novel Synthesis and Properties *ACS Nano* **4** 1539–44

[9] Jin C, Lin F, Suenaga K and Iijima S 2009 Fabrication of a Freestanding Boron Nitride Single Layer and Its Defect Assignments *Phys. Rev. Lett.* **102** 195505–4

[10] Warner J H, Rümmeli M H, Bachmatiuk A and Büchner B 2010 Atomic Resolution Imaging and Topography of Boron Nitride Sheets Produced by Chemical Exfoliation *ACS Nano* **4** 1299–304

[11] Qiao J, Kong X, Hu Z-X, Yang F and Ji W 2014 High-mobility transport anisotropy and linear dichroism in few-layer black phosphorus *Nat. Commun.* **5** 4475–82

[12] Zhu Z and Tománek D 2014 Semiconducting Layered Blue Phosphorus: A Computational Study *Phys. Rev. Lett.* **112** 176802–5

[13] Schusteritsch G, Uhrin M and Pickard C J 2016 Single-Layered Hittorf's Phosphorus: A Wide-Bandgap High Mobility 2D Material *Nano Lett.* **16** 2975–80

[14] Guan J, Liu D, Zhu Z and Tománek D 2016 Two-Dimensional Phosphorus Carbide: Competition between sp 2 and sp 3 Bonding *Nano Lett.* **16** 3247–52

[15] Miao N, Xu B, Bristowe N C, Zhou J and Sun Z 2017 Tunable Magnetism and Extraordinary Sunlight Absorbance in Indium Triphosphide Monolayer *J. Am. Chem. Soc.* **139** 11125–31

[16] Jing Y, Ma Y, Li Y and Heine T 2017 GeP3: A Small Indirect Band Gap 2D Crystal with High Carrier Mobility and Strong Interlayer Quantum Confinement *Nano Lett.* **17** 1833–8

[17] Lu N, Zhuo Z, Guo H, Wu P, Fa W, Wu X and Zeng X C 2018 CaP 3 : A New Two-Dimensional Functional Material with Desirable Band Gap and Ultrahigh Carrier Mobility *J. Phys. Chem. Lett.* **9** 1728–33

[18] Sun S, Meng F, Wang H, Wang H and Ni Y 2018 Novel two-dimensional semiconductor SnP 3 : High stability, tunable bandgaps and high carrier mobility explored using first-principles calculations *J. Mater. Chem. A* **6** 11890–7

[19] Nicolosi V, Chhowalla M, Kanatzidis M G, Strano M S and Coleman J N 2013 Liquid Exfoliation of Layered Materials *Science (80-.).* **340** 1226419–1226419

[20] Kuc A and Heine T 2015 The electronic structure calculations of two-dimensional transition-metal dichalcogenides in the presence of external electric and magnetic fields *Chem. Soc. Rev.* **44** 2603–14

[21] Heine T 2015 Transition Metal Chalcogenides: Ultrathin Inorganic Materials with Tunable Electronic Properties *Acc. Chem. Res.* **48** 65–72

[22] Novoselov K S, Geim A K, Morozov S V., Jiang D, Katsnelson M I, Grigorieva I V., Dubonos S V. and Firsov A A 2005 Two-dimensional gas of massless Dirac fermions in graphene *Nature* **438** 197–200

[23] Gillen R and Maultzsch J 2017 Light-Matter Interactions in Two-Dimensional Transition Metal Dichalcogenides: Dominant Excitonic Transitions in Mono- and Few-Layer MoX$_2$ and Band Nesting *IEEE J. Sel. Top. Quantum Electron.* **23** 219–30

[24] Mak K F, Lee C, Hone J, Shan J and Heinz T F 2010 Atomically Thin MoS2 : A New Direct-Gap Semiconductor *Phys. Rev. Lett.* **105** 136805–4

[25] Splendiani A, Sun L, Zhang Y, Li T, Kim J, Chim C Y, Galli G and Wang F 2010 Emerging photoluminescence in monolayer MoS2 *Nano Lett.* **10** 1271–5

[26] Sun J, Li X, Guo W, Zhao M, Fan X, Dong Y, Xu C, Deng J and Fu Y 2017 Synthesis Methods of Two-Dimensional MoS2: A Brief Review *Crystals* **7** 198–209

[27] Paton K R, Varrla E, Backes C, Smith R J, Khan U, O'Neill A, Boland C, Lotya M, Istrate O M, King P, Higgins T, Barwich S, May P, Puczkarski P, Ahmed I, Moebius M, Pettersson H, Long E, Coelho J, O'Brien S E, McGuire E K, Sanchez B M, Duesberg G S, McEvoy N,

Pennycook T J, Downing C, Crossley A, Nicolosi V and Coleman J N 2014 Scalable production of large quantities of defect-free few-layer graphene by shear exfoliation in liquids *Nat. Mater.* **13** 624–30

[28] Coleman J N, Lotya M, O'Neill A, Bergin S D, King P J, Khan U, Young K, Gaucher A, De S, Smith R J, Shvets I V, Arora S K, Stanton G, Kim H-Y, Lee K, Kim G T, Duesberg G S, Hallam T, Boland J J, Wang J J, Donegan J F, Grunlan J C, Moriarty G, Shmeliov A, Nicholls R J, Perkins J M, Grieveson E M, Theuwissen K, McComb D W, Nellist P D and Nicolosi V 2011 Two-Dimensional Nanosheets Produced by Liquid Exfoliation of Layered Materials *Science (80-.).* **331** 568–71

[29] Zhou K-G, Mao N-N, Wang H-X, Peng Y and Zhang H-L 2011 A Mixed-Solvent Strategy for Efficient Exfoliation of Inorganic Graphene Analogues *Angew. Chemie Int. Ed.* **50** 10839–42

[30] Li L H, Chen Y, Behan G, Zhang H, Petravic M and Glushenkov A M 2011 Large-scale mechanical peeling of boron nitride nanosheets by low-energy ball milling *J. Mater. Chem.* **21** 11862–6

[31] Ling X, Lee Y H, Lin Y, Fang W, Yu L, Dresselhaus M S and Kong J 2014 Role of the seeding promoter in MoS2 growth by chemical vapor deposition *Nano Lett.* **14** 464–72

[32] Lee Y-H, Zhang X-Q, Zhang W, Chang M-T, Lin C-T, Chang K-D, Yu Y-C, Wang J T-W, Chang C-S, Li L-J and Lin T-W 2012 Synthesis of Large-Area MoS 2 Atomic Layers with Chemical Vapor Deposition *Adv. Mater.* **24** 2320–5

[33] Ma Y, Kuc A and Heine T 2017 Single-Layer Tl2O: A Metal-Shrouded 2D Semiconductor with High Electronic Mobility *J. Am. Chem. Soc.* **139** 11694–7

[34] Donohue P C and Young H S 1970 Synthesis, structure, and superconductivity of new high pressure phases in the systems GeP and GeAs *J. Solid State Chem.* **1** 143–9

[35] Gullman J and Olofsson O 1972 The crystal structure of SnP3 and a note on the crystal structure of GeP3 *J. Solid State Chem.* **5** 441–5

[36] Wu H-H, Huang H, Zhong J, Yu S, Zhang Q and Zeng X C 2019 Monolayer triphosphates MP3 (M=Sn, Ge) with excellent basal catalytic activity for hydrogen evolution reaction *Nanoscale* **11** 12210–9

[37] Niu F, Cai M, Pang J, Li X, Zhang G and Yang D 2019 A first-principles study: Adsorption of small gas molecules on GeP 3 monolayer *Surf. Sci.* **684** 37–43

[38] Zhang C, Jiao Y, He T, Ma F, Kou L, Liao T, Bottle S and Du A 2017 Two-dimensional GeP3 as a high capacity electrode material for Li-ion batteries *Phys. Chem. Chem. Phys.* **19** 25886–90

[39] Deng X, Chen X, Huang Y, Xiao B and Du H 2019 Two-Dimensional GeP 3 as a High Capacity Anode Material for Non-Lithium-Ion Batteries *J. Phys. Chem. C* **123** 4721–8

[40] Kresse G and Furthmüller J 1996 Efficient iterative schemes for ab initio total-energy calculations using a plane-wave basis set *Phys. Rev. B* **54** 11169–86

[41] Kresse G and Joubert D 1999 From ultrasoft pseudopotentials to the projector augmented-wave method *Phys. Rev. B* **59** 1758–75

[42] Perdew J P, Burke K and Ernzerhof M 1996 Generalized Gradient Approximation Made Simple *Phys. Rev. Lett.* **77** 3865–8

[43] Barbiellini B and Bansil A 2004 Dyson Orbitals, Quasi-Particle effects and Compton scattering *J. Phys. Chem. Solids* **65** 2031–4

[44] Cahangirov S, Topsakal M, Aktürk E, Şahin H and Ciraci S 2009 Two- and One-Dimensional Honeycomb Structures of Silicon and Germanium *Phys. Rev. Lett.* **102** 236804–4

[45] Krukau A V., Vydrov O A, Izmaylov A F and Scuseria G E 2006 Influence of the exchange screening parameter on the performance of screened hybrid functionals *J. Chem. Phys.* **125** 224106–5

[46] Anon 2015 First principles phonon calculations in materials science *Scr. Mater.* **108** 1–5

[47] Martyna G J, Klein M L and Tuckerman M 1992 Nosé–Hoover chains: The canonical ensemble via continuous dynamics *J. Chem. Phys.* **97** 2635–43

[48] Lee C, Yan H, Brus L E, Heinz T F, Hone J and Ryu S 2010 Anomalous Lattice Vibrations of Single- and Few-Layer MoS $_2$ *ACS Nano* **4** 2695–700

[49] Björkman T, Gulans A, Krasheninnikov A V. and Nieminen R M 2012 van der Waals Bonding in Layered Compounds from Advanced Density-Functional First-Principles Calculations *Phys. Rev. Lett.* **108** 235502–5

[50] Ziambaras E, Kleis J, Schröder E and Hyldgaard P 2007 Potassium intercalation in graphite: A van der Waals density-functional study *Phys. Rev. B* **76** 155425–10

[51] Ghorbani-Asl M, Borini S, Kuc A and Heine T 2013 Strain-dependent modulation of conductivity in single-layer transition-metal dichalcogenides *Phys. Rev. B* **87** 235434–6

[52] Ghorbani-Asl M, Kuc A, Miró P and Heine T 2016 A Single-Material Logical Junction Based on 2D Crystal PdS2 *Adv. Mater.* **28** 853–6

[53] Yamaguchi H, Blancon J-C, Kappera R, Lei S, Najmaei S, Mangum B D, Gupta G, Ajayan P M, Lou J, Chhowalla M, Crochet J J and Mohite A D 2015 Spatially Resolved Photoexcited Charge-Carrier Dynamics in Phase-Engineered Monolayer MoS $_2$ *ACS Nano* **9** 840–9

[54] Koichi Momma, Fujio Izumi 2011 VESTA 3 for three-dimensional visualization of crystal, volumetric and morphology data *J. Appl. Crstallogr.,* **44** 1272–6